ORIGINAL PAPER

Spectral Investigations on 2,3-Bis(chloromethyl)-1,4-Anthraquinone: Solvent Effects and Host–Guest Interactions

M. Umadevi · P. Vanelle · T. Terme · V. Ramakrishnan

Abstract Solvent effects on 2,3-bis(chloromethyl)-1,4-anthraquinone (DCMAQ) and the molecular recognition of DCMAQ in calix[8]arene were investigated using optical absorption and fluorescence emission techniques. Optical absorption spectra show n→π* band in 350–500 nm region. It also indicates that the dipole–dipole interaction and solvent reorganization energies are responsible for the observed features in different solvents. The observed quantum yield of DCMAQ in different solvents is due to the formation of intermolecular hydrogen bond and reorientation of solvent molecule in the excited state of DCMAQ. Excited state dipole moment of DCMAQ is calculated by solvatochromic data and it shows a higher excited state dipole moment than ground state dipole moment. Optical absorption and fluorescence studies of DCMAQ in calix[8]arene elucidate the evidence for the formation of complex between DCMAQ and calix[8]arene. The inclusion ratios and inclusion constant of the host–guest complexes are also determined.

Introduction

Anthraquinone is the most important quinone derivative of anthracene. Plants containing anthraquinones have been used for millennia as dyestuffs and purgatives [1]. Though quinones are found in plants and in a few animals, they usually are prepared by oxidation of aromatic amines, polyhydric phenols, and polynuclear hydrocarbons. Anthraquinone derivatives have various biochemical characteristics (bioactivities) and have the wide application for medicines, pesticides, etc. [2]. They are used principally in photographic dye chemicals, in medicine, as an antioxidant, in paints, varnishes, motor fuels, oils, pigments and in organic inhibitor. They play a vital role in paper industry as a catalyst to increase the pulp production yield and to improve the fiber strength through reduction reaction of cellulose to carboxylic acid [3, 4]. Anthraquinone glycosides from a number of plants (including *Aloe* (Liliaceae), *Rhamnus* (Rhamnaceae), *Cassia* (Fabaceae or Leguminosae)) are widely used as laxatives. The anthraquinone laxatives essentially irritate the bowel wall, provoking increased muscle contractions and peristaltic movements [5]. The anthraquinone derivative rhein is significantly antiseptic and is especially toxic to the enteric pathogen *Shigella dysenteriae* as well as to *Staphylococci* [6]. Moreover, many anthraquinones have been investigated for their anticancer potential [7].

The study of calixarene has been of continuing research interest in the areas of host–gust chemistry, inclusion compounds, organic catalysts, analytical chemistry and

M. Umadevi (✉)
Department of Physics, Mother Teresa Women's University,
Kodaikanal, 624 102, Tamil Nadu, India

P. Vanelle · T. Terme
Department of Organic Chemistry, UMR CNRS 6517,
University of Méditerranée, Faculty of Pharmacy,
27 Bd Jean Moulin,
13385 Marseille Cedex 5, France

V. Ramakrishnan
Department of Laser Studies, School of Physics, Madurai
Kamaraj University,
Madurai, 625 021, India

in supramolecular chemistry [8–11]. The pioneering work of C.D. Gutsche in the late 1970s led to a renewed interest in the chemistry of phenol–formaldehyde products, and his naming such products *calixarenes* [12, 13]. Calixarenes are macro-cyclic compounds composed of phenolic units connected by methylene bridges to form a hydrophobic cavity in several sizes. The functionalization of the upper rim, the lower rim or both and the conformation of the calixarene moiety determine the size and geometry of the host and therefore significantly change the selectivity of binding. Calixarenes with as few as three and as many as twenty repeating units are known. The majority of studies deal with derivatives of calix[4]arenes, calix[6]arenes, and calix[8]arenes due to the retention of the calixarene cavity [14].

Optical absorption and fluorescence emission techniques are good probes to study the nature and role of hydrogen bonding and inclusion phenomena of anthraquinone deriva-tives. Absorption spectra reveal the solvent–solute interac-tion, which can be predicted from the position, intensity, and shape of the absorption band. Fluorescence spectroscopy is a powerful method for studying the characterization of excited states such as exciplex formation, excited state intramolec-ular proton transfer reaction, solvent interaction, hydrogen bonding, fluorophore conformation, binding sites, degree of flexibility, internal motions and many other physicochemi-cal parameters [15]. Several groups have investigated solvent effects on anthraquinone derivatives [16–22]. Host–guest in-teraction of calixarene and quinone derivatives have also been reported [23, 24].

In the present study, optical absorption and fluorescence emission spectroscopic techniques were employed to in-vestigate the solvent effects on 2,3-bis(chloromethyl)-1,4-anthraquinone (DCMAQ), excited state dipole moment of DCMAQ and the molecular recognition of DCMAQ in calix[8]arene.

Experimental

DCMAQ was prepared from 1,4-anthraquinone according to Thomson's procedure [25]. A solution of 1,4-anthraquinone (2.6 g, 12.48 mM) in glacial acetic acid (50 ml) containing aqueous formaldehyde (20 ml, 37%) was cooled and dry hydrogen chloride passed through it for 2 h. The mixture was allowed to stand at room temperature overnight and was poured into 200 ml of ice water. The product was collected by filtration, washed with water and dried over anhydrous magnesium sulfate. Purification by chromatography on sil-ica gel eluting with dichloromethane gave DCMAQ in 61% yield.

Calix[8]arene was prepared from *p-tert*-butyl phenol and formaldehyde according to the literature [26]. In brief, 30 g of *p-tert*-butyl phenol and 9.5 g of formaldehyde were dissolved

in 150 ml of xylene. The mixture was refluxed at 120 °C for about 4 h in an inert atmosphere to get a pale brown colored precipitate. It was washed with suitable solvents and recrystallized to get a pure white powder (calix[8]arene) (Scheme 1).

For solvent effects on DCMAQ, carbon tetrachloride, dichloromethane, propan-2-ol, methanol and acetonitrile from Sisco laboratory with 99% purity were used without further purification. The concentration of DCMAQ in the above-mentioned solvents was 0.08 mM for optical absorp-tion and fluorescence measurements.

Dichloromethane was used as the solvent for inclu-sion studies of DCMAQ in calix[8]arene. For the Job's plot of continuous variation, optical absorption and fluo-rescence spectra were measured for varying concentrations of both calix[8]arene and DCMAQ, keeping the total con-centration constant. (i.e. $[H] + [G] = 0.8$ mM). To find out association constant, optical absorption spectra were measured for different concentration of calix[8]arene from 0.008 mM to 0.08 mM keeping DCMAQ concentration con-stant (0.04 mM).

All optical absorption spectra were recorded with an UV-160 Shimadzu spectrophotometer of resolution ± 0.5 nm. Fluorescence spectral measurements were made by employ-ing the experimental arrangement used in our laboratory [27]. SPECTRA PHYSICS 2020-04S argon ion laser was used as a source of excitation. The scattered light was dispersed with a grating monochromator and detected with a thermoelectri-cally cooled RCA GaAs photo multiplier tube. A PC was interfaced through a data acquisition add-on card to record the spectra. The 457.9 nm line of argon ion laser was used as the excitation wavelength and the power at the sample was maintained at 15 mW. The resolution of the instrument was ± 0.1 nm. All the experiments were carried out at room temperature.

Parker's method was employed to determine the rela-tive fluorescence quantum yield (φ_{rel}) [28] in which 1-methylamino anthraquinone in benzene was used as fluo-rescence standard ($\varphi = 0.76 \times 10^{-2}$) [29].

Results and discussion

Solvent effects on DCMAQ

Optical absorption spectral studies

The structural formula of DCMAQ is presented in Fig. 1. The absorption spectra of DCMAQ in different solvents are shown in Fig. 2. The spectra show a single broad band in the region 350–500 nm which is due to $n \rightarrow \pi^*$ transition [30]. As the solvent polarity increases the peaks are red shifted except in the case of methanol. In methanol there is no shift in peak

Scheme 1

p-tert-butyl phenol (formaldehyde)$_8$ calix(8)arene

calix(8)arene
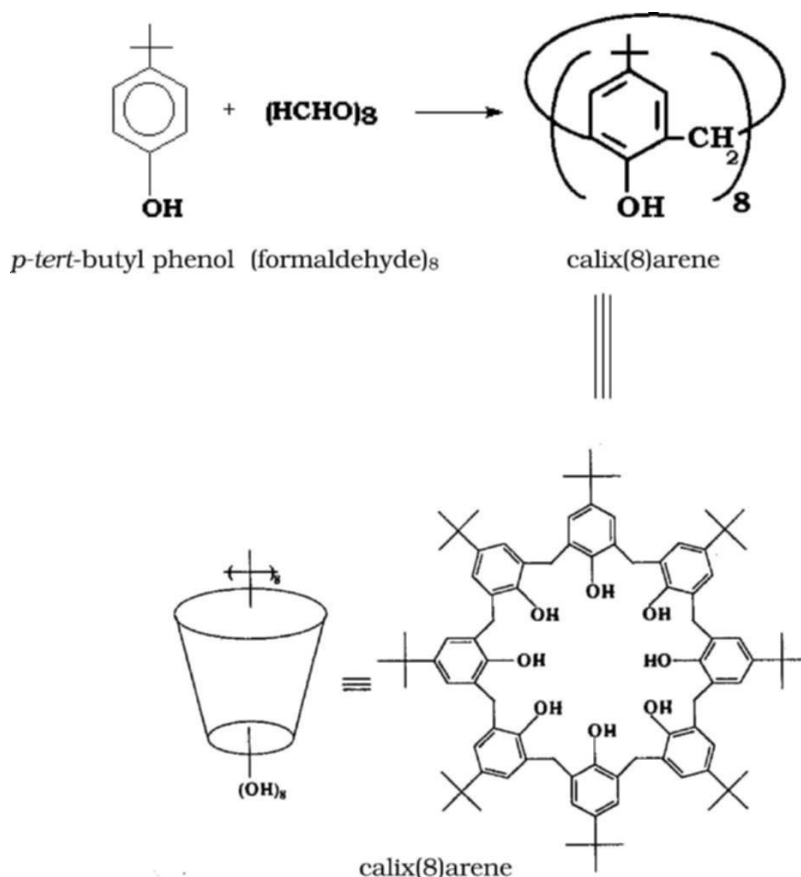
with respect to the apolar (carbon tetrachloride) solvent. In dichloromethane, the shift is 8 nm and in propan-2-ol and acetonitrile it is 3 nm.

Generally, the band due to an $n \rightarrow \pi^*$ transition suffers a blue shift in more polar solvents due to the lower dipole moment of the singlet excited state with respect to the ground state [31]. In anthraquinone derivatives, the features observed for the $\pi\pi^*$ band generally mask that of the $n\pi^*$ band owing to its high intensity. It is generally explained in terms of the hydrogen bonding and charge transfer between the substituent and the carbonyl group or the intramolecular hydrogen bonded carbonyl chelated ring [32]. The observed red shift shows that this band may be masked by high intense $\pi\pi^*$ band occur at 242 nm (not shown in Fig. 2) which undergoes a red shift due to the high dipole moment in the excited state [21].

Fig. 1 Structural formula of 2,3-bis(chloromethyl)-1,4-anthraquinone
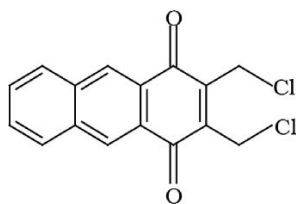
The wavelength of maximum intensity and full width at half maximum (FWHM) of a band are characteristics of the absorption spectrum. The FWHM value of the absorption band shows a variation of $500\,\mathrm{cm^{-1}}$ in dichloromethane, $860\,\mathrm{cm^{-1}}$ in propan-2-ol, $54\,\mathrm{cm^{-1}}$ in methanol and $752\,\mathrm{cm^{-1}}$ in acetonitrile with respect to carbon tetrachloride. The observed high FWHM value for the solvent methanol indicates a strong association of solvent molecules with DCMAQ in the ground state via the formation of intermolecular hydrogen bonds between the hydroxyl group of the alcohol and the quinoid oxygen. In the case of amino anthraquinone (anthraquinone with electron donating/withdrawing substituents), the strength of inter molecular hydrogen bond in the excited state is confirmed by reported solvatochromic data, indicating a significant red shift of the absorption peak for increasing solvent polarity [32, 33]. In the present case, the strength of the hydrogen bond remains the same in the excited state owing to neutral substituents. Even though intermolecular hydrogen bond formed in propan-2-ol, the steric effect due to the methyl groups in propan-2-ol is responsible for the observed FWHM in propan-2-ol. In acetonitrile, FWHM value decreases by $752\,\mathrm{cm^{-1}}$ with respect to carbon tetrachloride, which indicates a strong association of solvent molecule and DCMAQ in the excited state by dipole–dipole interaction with respect to ground state.
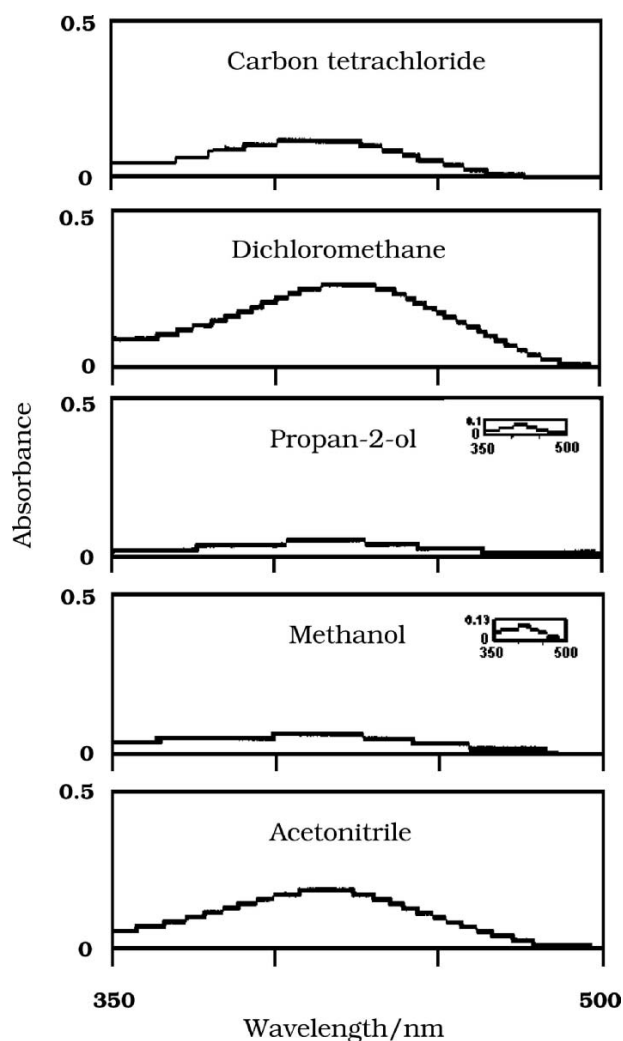
Fig. 2 Optical absorption spectra of DCMAQ in different solvents (inset: expanded spectrum)

As the substituents are neutral, the effect of substituents on the optical absorption characteristics is negligible as compared with electron-donating/withdrawing substituents [35].

Fluorescence spectral studies

The fluorescence emission spectra of DCMAQ in different solvent show two peaks, which is shown in Fig. 3. It is observed with intensity maxima at 541 and 564 nm in carbon tetrachloride, 541 and 568 nm in dichloromethane, 531 and 564 nm in propan-2-ol, 530 and 555 nm in methanol and 535 and 564 nm in acetonitrile. It also shows that the short wavelength peaks are more prominent than the long wavelength peak in all solvents except in acetonitrile.

The observed more prominent short wavelength peak in propan-2-ol and methanol are due to the methyl group in the solvent molecules. It is confirmed by measuring the wavelength difference between λ_{ext} and λ_{max1} of propan-2-ol and
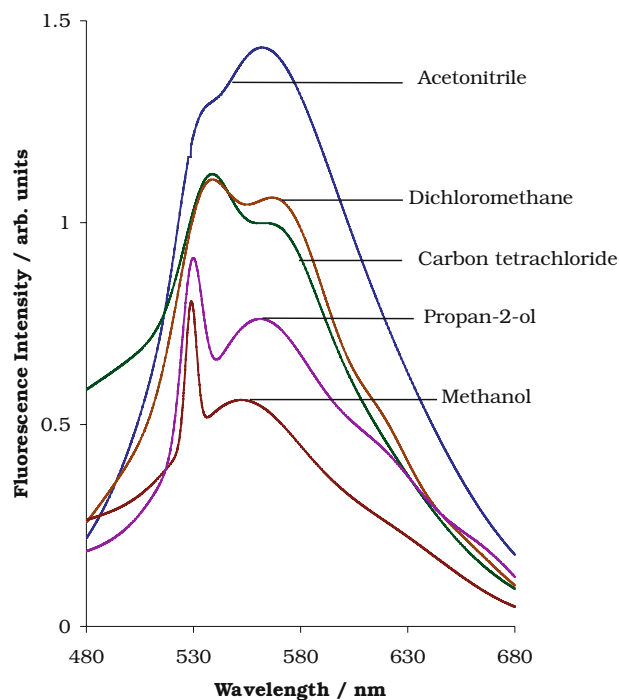

Fig. 3 Fluorescence emission spectra of DCMAQ in different solvents ($\lambda_{ext} = 457.9$ nm)

methanol. It is around 2980 cm^{-1}, which is due to asymmetric stretching of methyl group [36]. As the solvent polarity increases, the short and long wavelength peaks are blue shifted with respect to apolar solvent on contrary to the generally observed red shift.

Examination of the spacing between the vibrational structure reveals that a vibrational mode initiates the progression of peaks. This value is 808, 875, 1090, 844 and 971 cm^{-1} in carbon tetrachloride, dichloromethane, propan-2-ol, methanol and acetonitrile respectively. This gives rise to C–H out-of-plane bending progression of anthraquinone in carbon tetrachloride, dichloromethane, methanol and acetonitrile and ring deformation progression of anthraquinone in propan-2-ol.

The observed blue shift in polar solvent reveals that DCMAQ is more stabilized in the ground state. In the case of polar protic solvents (methanol and propan-2-ol), the ground state is more stabilized by intermolecular hydrogen bond between the hydroxyl group of the solvents and the quinoid oxygen. The strength of this bond remains same in the excited state due to the neutral substituent of DCMAQ. In the case of polar aprotic solvents (dichloromethane and acetonitrile), the observed red shift indicates the reorientation of solvent molecule around the excited state dipole gives rise to a minor effect.

The relative fluorescence quantum yields were calculated for DCMAQ in the above-mentioned solvents and were listed in Table 1. It shows a lower quantum yield in polar protic

Table 1 Fluorescence quantum yield (φ_{rel}) of DCMAQ in different solvents

Solvents	φ_{rel} ($\times 10^{-3}$)
Carbon tetrachloride	1.33
Dichloromethane	4.87
Propan-2-ol	0.64
Methanol	0.44
Acetonitrile	2.89

solvents with respect to polar aprotic and apolar solvents. In polar protic solvents, OH group of these solvents have the tendency to form an intermolecular hydrogen bonding with a C=O group of anthraquinone ring. The intermolecular hydrogen bond OH⋯O=C acts as an acceptor mode which increases the non-radiative decay and gives rise to a lower quantum yield in polar protic solvents. The polar aprotic solvents show a high quantum yield with respect to apolar solvent. The reorientation of solvent molecule around excited state dipole increases radiative decay, which in turn increases the fluorescence quantum yield in polar aprotic solvents.

Dipole moment of the excited state

The effect of solvent on absorption spectra of molecules can be used to determine the magnitude as well as direction of electric dipole moment of solute molecule in its first electronically excited state. The study of this parameter helps to understand electronic charge distribution, reactivity etc. of the solute molecule in its first electronically excited state [37, 38].

It is well established from [39–41] that the bulk dielectric constant (ε) and refractive index (n) of solvent play major roles in effecting dipole moments of solute molecules. An interaction with environment e.g. solvent, temperature etc. affects differently in various electronic states. The universal interaction between solute and solvent molecules is due to solvent acting as a dielectric medium. It also depends upon dielectric constant, refractive index of the solvent and dipole moment of the solute molecules.

According to Bakshiev [42], Chamme and Viallet [43]

$$\bar{v}_a - \bar{v}_f = m_1 F_1(\varepsilon, n) + C_1 \tag{1}$$

$$\overline{v_a} + \overline{v_f} = -m_2 F_2(\varepsilon, n) + C_2 \tag{2}$$

where $\bar{v}_a$ and $\bar{v}_f$ are absorption maximum and fluorescence maximum and $F(\varepsilon, n)$ is the solvent polarity parameter.

$$F_1(\varepsilon, n) = \left(\frac{\varepsilon - 1}{\varepsilon + 2} - \frac{n^2 - 1}{n^2 + 2} \right) \left(\frac{2n^2 + 1}{n^2 + 2} \right) \tag{3}$$

$$F_2(\varepsilon, n) = F_1(\varepsilon, n) + 2G(n) \tag{4}$$

$$G(n) = \frac{3}{2} \frac{(n^4 - 1)}{(n^2 + 2)^2} \tag{5}$$

where ε is dielectric constant and n is refractive index of the solvent.

$$m_1 = \frac{2(\mu_e - \mu_g)^2}{hca^3} \tag{6}$$

$$m_2 = \frac{2(\mu_e^2 - \mu_g^2)}{hca^3} \tag{7}$$

where μ_e and μ_g are excited state and ground state dipole moment of solute molecules respectively, h is the Planck's constant, c is the velocity of light and a is Onsager cavity radius.

From Eqs. (6) and (7), the ratio of dipole moments in excited and ground state is given by

$$\frac{\mu_e}{\mu_g} = \left| \frac{m_1 + m_2}{m_2 - m_1} \right| \tag{8}$$

The photophysical parameters deduced from the observed absorption and emission spectra of DCMAQ in different solvents are tabulated in Table 2. Fig. 4 shows correlation between $\bar{v}_a - \bar{v}_f$ and $F_1(\varepsilon, n)$ and Fig. 5 shows correlation between $\bar{v}_a + \bar{v}_f$ and $F_2(\varepsilon, n)$ (by eliminating the dichloromethane data which shows much deviation, linear plot has been drawn). It can be seen that, the dichloromethane solvent shows much deviation from linear plot. This deviation from linearity may be due to specific solute–solvent interaction [44]. The ratio of dipole moments in excited state and ground state for the present case is found to be 3.78.

The following conclusion has been drawn from the dipole moment determination using solvent polarity parameter

1. The polarity of a molecule depends on electron density. With supply of additional energy there will be transition of electron from ground state to excited state. Due to the movement of electron from ground state orbital to higher level orbital there will be increase of dipole moment with reference to ground state dipole moment. Therefore in general the values of the excited state dipole moments are higher than the ground state dipole moments.

2. The observed red shift (absorption maximum) in polar solvent provides the evidence for the observed dipole moment of the excited state, which is greater than dipole moment of the ground state.

3. The observed smaller slope values (m_1 and m_2) indicating a rather small variation of the dipole moment values between the ground state and excited state. This suggests that the emission of DCMAQ originates from a state, which although more polar than the ground state, is probably a locally excited intramolecular charge transfer state.

Table 2 Photo physical parameters of DCMAQ deduced from optical absorption and fluorescence measurements

Solvents	λ_a (nm)	λ_f (nm)	$\bar{v}_a - \bar{v}_f$ (cm^{-1})	$\bar{v}_a + \bar{v}_f$ (cm^{-1})	$F_1(\varepsilon, n)$	$F_2(\varepsilon, n)$
Carbon tetrachloride	412.7	540.7	5736	42725	0.02	0.64
Dichloromethane	421.2	541.0	5257	42226	0.59	1.17
Propan-2-ol	415.5	531.0	5235	42900	0.77	1.28
Methanol	412.7	529.8	5356	43106	0.86	1.30
Acetonitrile	415.5	534.7	5365	42769	0.86	1.33

Change transfer accompanying excitation to the lowest excited state usually results in the excited molecule having a greater dipole moment than the one in ground state [44]

4. In addition the observed less pronounced absorption shift with solvent implies that the ground state energy distribution is not affected to a greater extent possibly due to the less polar nature of the dye in the ground state rather than the excited state [45].

Molecular recognition of DCMAQ by calix[8]arene

Optical absorption spectral studies

Figure 6 shows the absorption spectra of calix[8]arene and DCMAQ solution in varying molar ratios of two different components keeping the sum of both concentration equal to 0.8 mM. It shows sharp peak around 240 nm and broad peaks around 275 and 420 nm. It shows a hypochromicity effect in the DCMAQ rich region. The bands around 240 and 275 nm show a blue shift and red shift in calix[8]arene rich region respectively. As the concentration of calix[8]arene increases the peak observed at 275 nm is disappeared and a new peak is observed at 292 nm.

In the present case, the lack of isosbestic point suggests that multiple-site binding and dye aggregation may occur within the used range of concentration [46].

Anthraquinone derivatives have four $\pi\pi^*$ absorption bands in the region of the wavelength between 220–350 nm

and an $n\pi^*$ band at longer wavelength near 400 nm [30]. The observed bands around 240 and 270 nm are assigned to $\pi\pi^*$ band and the band at 420 nm is assigned to $n\pi^*$ band.

The observed absorption spectral features around 275 nm band of DCMAQ in the presence calix[8]arene reflect the extent of complexation and make it possible to determine the binding constant.

The main contribution to the variation of host–guest interaction must come from polar interaction and more significantly hydrogen bonding of the guest with host molecules. The observed red shift in calix[8]arene rich region indicates that the excited states formed by transition is in extremely polar state and it is also due to the intermolecular hydrogen bond formation between OH group of calix[8]arene and C=O group of DCMAQ.

The stoichiometries of the complexes were determined by the Job method of continuous variations. A continuous variation plot of ΔA_{274} vs mole fraction of calix[8]arene ($[H]/([H] + [G])$ where $[H] + [G] = 0.8$ mM) (Fig. 7) gave a minimum value at 0.2, indicating the formation of a 1:4 complex. Generally continuous variation plot shows a maximum ΔA at a particular mole fraction of host which provides the stoichiometries of the complex formation i.e. absorbance value of the complex is higher than that of free guest [47]. In the present case, we observed a lower absorbance value in the complex when compared to free guest due to the intermolecular hydrogen bond formation between guest and host.
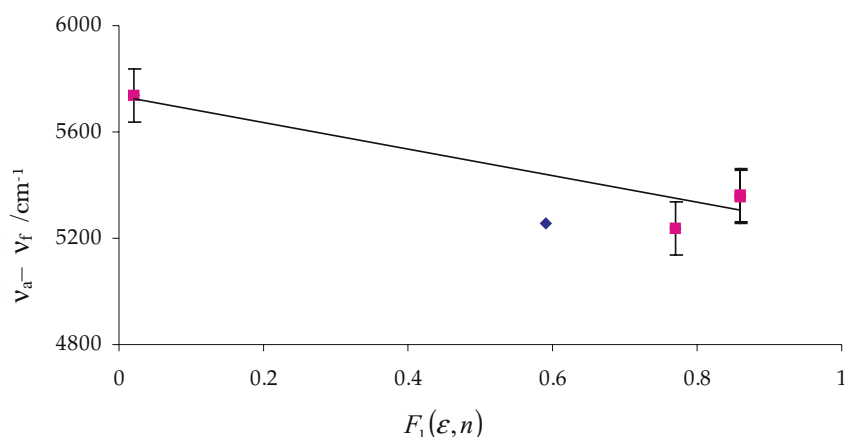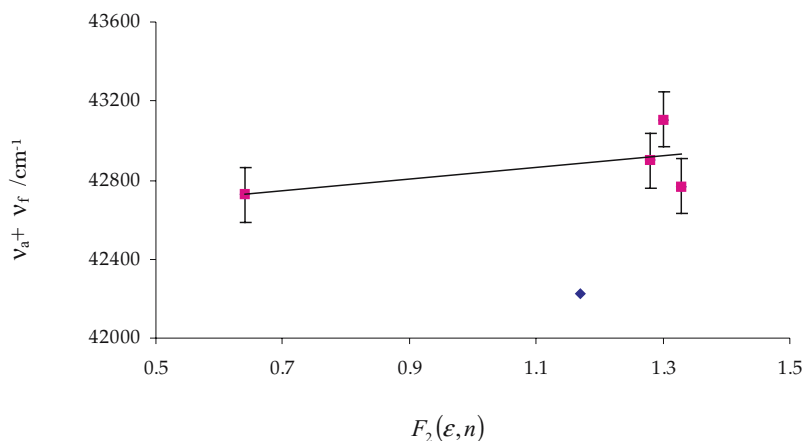
Fig. 4 Plot of $\bar{v}_a - \bar{v}_f$ against polarity function $F_1(\varepsilon, n)$

Fig. 5 Plots of $\bar{\nu}_a + \bar{\nu}_f$ against polarity function $F_2(\varepsilon, n)$

The inclusion constant K for DCMAQ-calix[8]arene complex was determined using the Benesi–Hildebrand equation [48] which has been deduced as

$$\frac{[G]}{A} = \frac{1}{K\alpha[H]^n} + \frac{1}{\alpha} \tag{9}$$

where $[G]$ is the concentration of guest (DCMAQ), A is the absorptivity at 273.5 nm, $[H]$ is the concentration of host (calix[8]arene), α is the constant and n is the number of host molecules in a complex. By plotting the $[G]/A$ vs $1/[H]^n$ graph with different n, the n that results a straight line can be taken as the number of host molecules, consequently, the inclusion ratio can be obtained as $1:n$ [49–51]. From the intercept and the slop of the straight line, the inclusion constant can be obtained. Fig. 8, shows that the inclusion constant K is equal to 529 M^{-1} and the linearity of the plot indicates that the composition ratio of the inclusion complex is 1:4 for calix[8]arene:DCMAQ.

Fluorescence spectral studies

The emission spectra of calix[8]arene and DCMAQ solution in varying molar ratios of two components keeping the sum of both concentration equal to 0.8 mM is shown in Fig. 9. It shows a broad and featureless band around 526 nm in calix[8]arene rich region and it is weakly structured as the concentration of DCMAQ increases. This appears to be a structured band in DCMAQ rich region and the patterns are similar to that of the free DCMAQ. As the concentration of DCMAQ increases (DCMAQ rich region) a hyperchromicity effect is observed and it is maximum at 1:4 molar ratio of calix[8]arene/DCMAQ.

Generally an iso-emissive point is observed in the fluorescence spectra indicating that there are two species in equilibrium providing clear evidence for the following equilibrium [52]
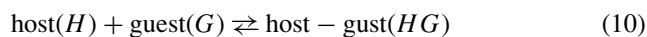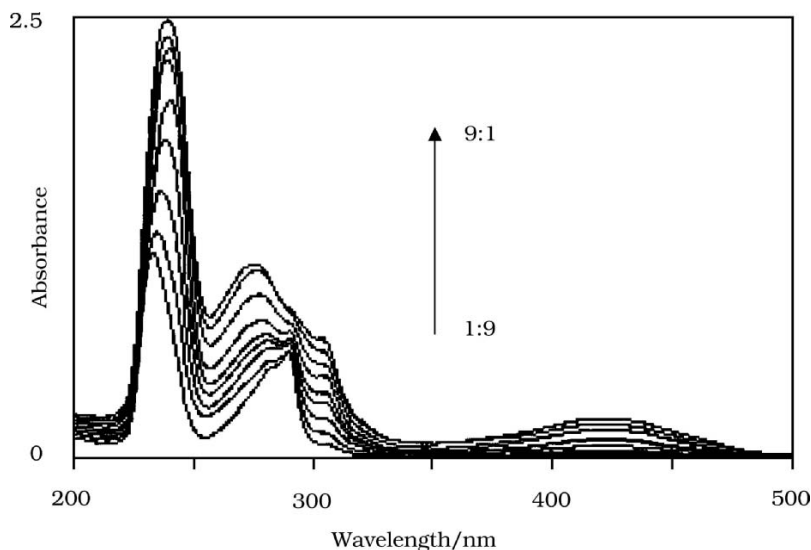
$$\text{host}(H) + \text{guest}(G) \rightleftarrows \text{host} - \text{gust}(HG) \tag{10}$$

Fig. 6 Optical absorption spectra of calix[8]arene—DCMAQ in different molar ratio (DCMAQ:calix[8]arene) keeping $[H] + [G] = 0.8$ mM (Dichloromethane is used as a solvent)
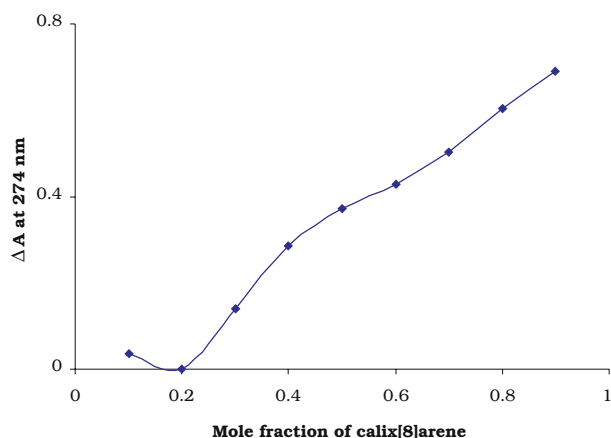
Fig. 7 Variation of ΔA at 274 nm with the mole fraction of calix[8]arene (keeping $[H]+[G]=0.8$ mM) (Dichloromethane is used as a solvent)

The lack of an iso-emissive point in the fluorescence spectra could suggest the formation of more than one DCMAQ-calix[8]arene inclusion complex.

The emission maximum occurs at 541 nm in the absence of calix[8]arene are blue shifted upon addition of calix[8]arene and the shift is minimum in the DCMAQ rich region and it is maximum in the calix[8]arene rich region.

Generally larger red shifts are observed in polar solvents than in a apolar solvents, indicating that the excited states of the anthraquinone are more stabilized by polar solvents [29]. Anthraquinone derivatives in polar protic solvents show red shift in the emission peak with respect to apolar solvent which is due to loss of energy by intermolecular hydrogen bond formation between carbonyl group of anthraquinone and hydroxyl group of solvent. The observed blue shift in the emission peak in calix[8]arene rich region indicating a weak interaction between calix[8]arene and DCMAQ. In DCMAQ rich region, blue shift is less indicating a strong interaction between calix[8]arene and DCMAQ through intermolecular
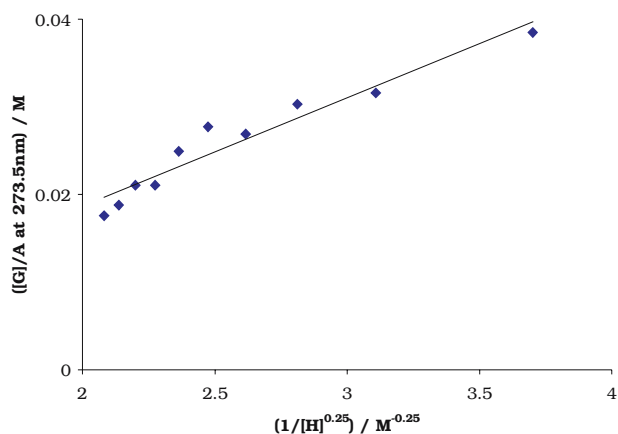

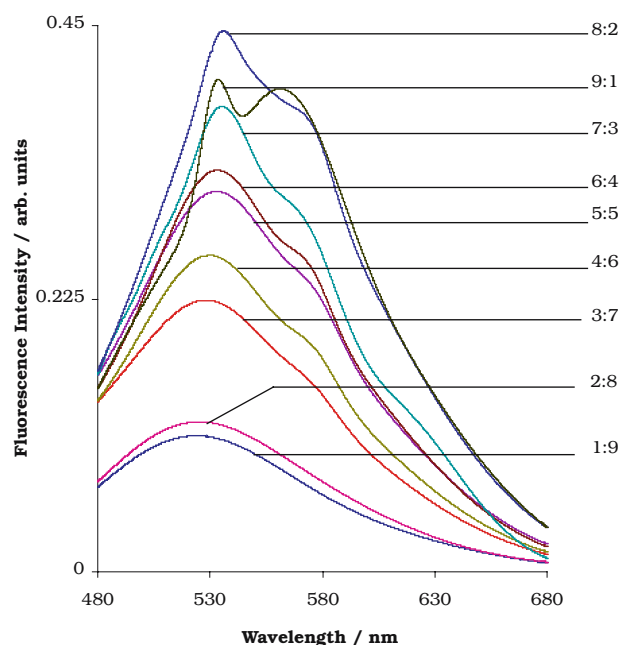**Fig. 8** Variation of [G]/A at 273.5 nm with $1/[H]^{.25}$ (Dichloromethane is used as a solvent)

Fig. 9 Fluorescence emission spectra of calix[8]arene—DCMAQ in different molar ratio (DCMAQ: calix[8]arene) keeping $[H]+[G]=0.8$ mM ($\lambda_{ext}=457.9$ nm) (Dichloromethane is used as a solvent)

hydrogen bond between OH group of calix[8]arene lower rim and C=O group of DCMAQ. An important factor in the blue shift of the emission peaks in calix[8]arene could be due to the stabilization of the ground state by intermolecular hydrogen bonding between calix[8]arene and DCMAQ and it also suggests that the anthraquinone rings are in more apolar region [53].

The relative fluorescence quantum yields are estimated and listed in Table 3. Binding to the calix[8]arene causes quenching of fluorescence as indicated by the observed fluorescence quantum yields. The dependence of F/F_0 on the mole fraction of calix[8]arene exhibits the maximum at 1:4 molar ratio of calix[8]arene/DCMAQ (Fig. 10), confirming the 1:4 stoichiometry of the complexes (F_0 and F are the integral fluorescence intensities of DCMAQ in the absence and presence of calix[8]arene respectively).

Table 3. Fluorescence quantum yield (φ_{rel}) of calix[8]arene and DCMAQ complexes

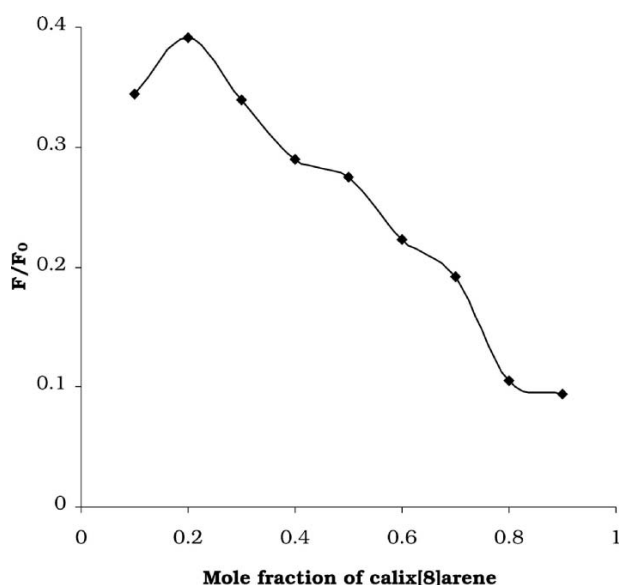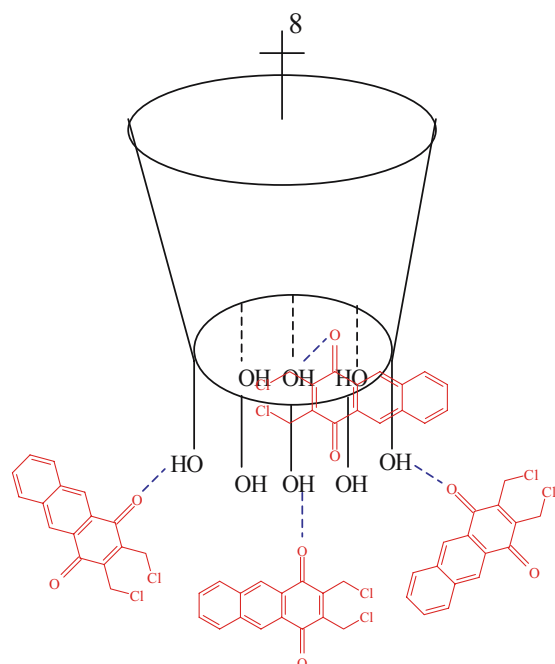| DCMAQ: calix[8]arene (Molar ratio)	φ_{rel} ($\times 10^{-3}$)
1:9	0.02
2:8	0.07
3:7	0.22
4:6	0.37
5:5	0.57
6:4	0.75
7:3	0.90
8:2	1.19
9:1	1.18

Fig. 10 Variation of F/F_0 with the mole fraction of calix[8]arene (keeping $[H] + [G] = 0.8$ mM) ($\lambda_{ext} = 457.9$ nm) (Dichloromethane is used as a solvent)

The molecular dimension of calix[8]arene is 3×11.7 Å [23] and the molecular dimension of DCMAQ is 10.4×5.4 Å determined by Chem 3D. Since the size of the calix[8]arene is small to adopt one DCMAQ, it is impossible to adopt four DCMAQ by a calix[8]arene cavity. The observed 1:4 stoichiometric ratio and the fluorescence quantum yield suggest that the four guest molecules are bound to the calix[8]arene

via intermolecular hydrogen bond between the OH group of calix[8]arene and C=O group of DCMAQ which efficiently quenches the fluorescence of DCMAQ.

There are two different ways by which DCMAQ can bound to calix[8]arene. (i) The four guest molecules are attached to the lower rim of the calix[8]arene and (ii) the guest molecules may bound to the walls of the calix[8]arene. In the first case (Scheme 2a) intermolecular hydrogen bond formed between the OH group of calix[8]arene and C=O group of DCMAQ shows a dominating effect for the observed fluorescence quantum yield. In the second case (Scheme 2b) the following interactions are possible between calix[8]arene and DCMAQ, (a) Intermolecular hydrogen bond between the OH group of calix[8]arene and C=O group of DCMAQ, (b) $\pi-\pi$ interaction between the benzene rings of calix[8]arene and anthraquinone ring [54], (c) CH–π interaction between the CH group in the substituent of DCMAQ and π system of

Scheme 2a Optimized structure of Calix[8]arene—DCMAQ complexes
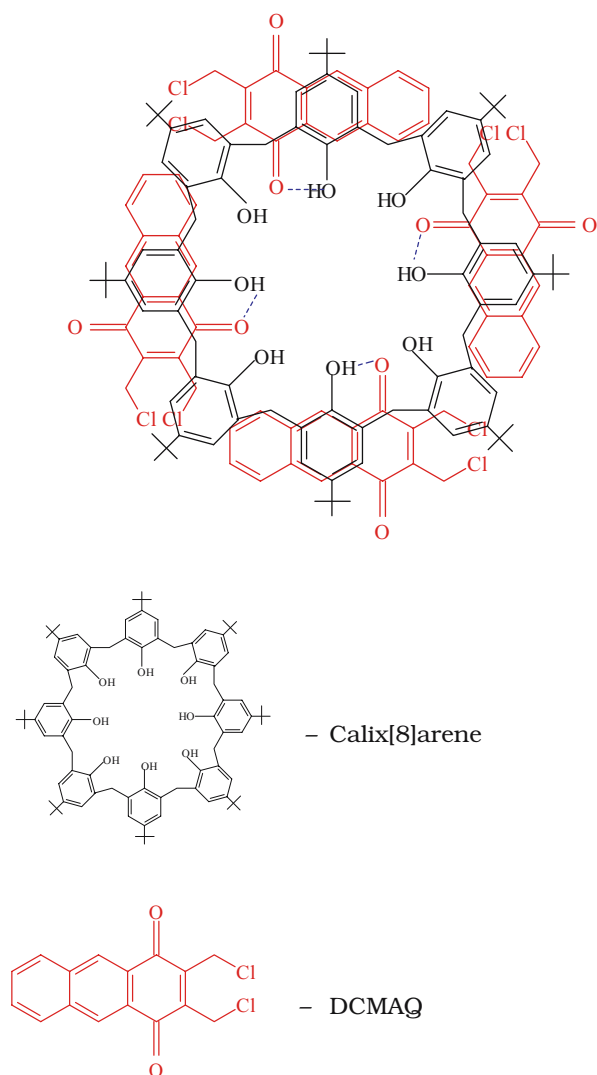
Scheme 2b Optimized structure of Calix[8]arene—DCMAQ complexes

the calix[8]arene [55] and (d) π arene$\cdots$H bonding between the hydrogen atom of the substituent in DCMAQ which may point directly towards the center of the aromatic ring of the calix[8]arene [56]. All these driving forces for complex formation are generally stabilize the host–guest complex and they are responsible for the non-radiative decay of fluorescence emission with respect to free DCMAQ.

The observed higher quantum yield in 1:4 ratio of calix[8]arene and DCMAQ indicates that at this ratio, a weak intermolecular hydrogen bond formed between the OH group of calix[8]arene and C=O group of DCMAQ and hence most probably DCMAQ may bound to the benzene ring of the calix[8]arene by π–π interaction.

Conclusion

Optical absorption and fluorescence emission studies on DCMAQ were carried out to study the solvent effect on DCMAQ and host–guest interaction of DCMAQ with calix[8]arene. Dipole–dipole interaction, solvent reorganization energies and intermolecular interactions are responsible for the observed features in the optical absorption and fluorescence emission spectra. Excited state dipole moment of DCMAQ was higher than that of ground state dipole moment determined using solvatochromism method. The inclusion ratios and inclusion constant of the host–guest complexes are determined using optical absorption and fluorescence emission techniques.

References

1. Hirsikorpi M, Kamarainen T, Teeri T, Hohtola A (2002) Plant Sci 162:537
2. Yanzhu L, Min D, Ziweri S (1999) Tsinghua Scie Tech 4:4
3. Jahan MS (2001) Tappi J 84:61
4. Li Z, Li J, Kubes GJ (2002) J Pulp Paper Sci 28:234
5. Mahulol University Annual Research Abstract (2001) 28:185
6. Brown JR, Imam SH (1984) Prog Mag Chem 21:196
7. Hua DH, Lou K, Havens J, Perchellet EM, Wang Y, Perchellet JP, Iwamoto T (2004) Tetrahedron 60:10155
8. Arimura T, Kawabata H, Matsuda T, Muramatsu T, Satoh H, Fugio K, Manabe P, Shinkai S (1991) J Org Chem 56:301
9. Atwood JW, Koptsantonis GA, Raston CL (1994) Nature 368:229
10. Araki K, Yanagi A, Shinkai S (1993) Tetrahedron 49:6763
11. Yamamoto H, Shinkai S (1994) Chem Lett 1115
12. Baekeland LH (1908) US Patent 942:699
13. Gutsche CD, Dhawan B, No KH, Muthukrishnan RJ (1981) J Am Chem Soc 103:3782
14. Stewart DR, Gutsche CD (1999) J Am Chem Soc 121:4136
15. Valeur B (2000) Molecular Fluorescence Principles and Applications, Wiley–Vch
16. Reta MR, Cattana R, Anunziata JD, Silber JJ (1993) Spectrochim Acta 49A:903
17. Yakovlev Yu, Nurmukhametov RN, Klimenko VG, Barashkov NN (1990) J Appl Spectrosc 53:53
18. Inoue H, Hida M, Nakashlma N, Yoshlhara K (1982) J Phys Chem 86:3184
19. Flom SR, Barbara PF (1985) J Phys Chem 87:4487
20. Umadevi M, Ramakrishnan V (2002) Spectrochim Acta 58A:2941
21. Umadevi M, Ramakrishnan V (2003) Spectrochim Acta 59A:393
22. Umadevi M, Ramakrishnan V (2002) J Raman Spectrosc 34:13
23. Chawla HM, Srinivas K, Meena S (1995) Tetrahedron 51:2709
24. Umadevi M, Ramasubbu A, Vanelle P, Ramakrishnan V (2003) J Raman Spectrosc 34:112
25. Thomson RH (1953) J Chem Soc 1196
26. Munch JM, Gutsche CD (1990) Org Synth 68:243
27. Jayaraj SE, Ramakrishnan V (1995) Spectrochim Acta 51A:979
28. Parker CA, Rees WT (1960) Analyst 85:587
29. Inoue H, Hida M, Nakashlma N, Yoshlhara K (1982) J Phys Chem 86:3184
30. Yoshida Z, Takabayashi F (1968) Tetrahedron 24:913
31. Singh AK, Bhasikuttan AC, Palit DK, Mittal JP (2000) J Phys Chem 104A:7002
32. Smulevich G, Angeloni L, Giovannardi S, Marzocchi MP (1982) J Chem Phys 65:313
33. Palit DA, Pal H, Mukherjee T, Mittal JP (1990) J Chem Soc Faraday Trans 86:3861
34. Marrucci L, Paparo D, Vetrano MR, Colicchio M, Santamato E, Viscardi G (2000) J Chem Phys 113:10361
35. Bhasikuttan AC, Singh AK, Palit DK, Sapre AV, Mittal JP (1998) J Phys Chem 102A:3470
36. Colthup NB, Daly LH, Wilberley SE (1990) Introduction to infrared and Raman Spectroscopy, Academic Press, New York
37. Medhi RN, Barman R, Medhi KC, Jois SS (1998) Spectrochim Acta 54A:623
38. Kumar S, Rao VC, Rastogi RC (2001) Spectrochim Acta 57A:41
39. Prabhmirachi LS, Kutty DKN, Bhide AS (1983) Spectrochimica Acta 39A:663
40. Suppan P (1983) Chem Phys Lett 94:272
41. Bakshiev NG (1962) Opt Spectrosc 13:507
42. Bakshiev NG (1964) Opt Spectrosc 16:821
43. Chamma A, Viallet P, Hebd CR (1970) Seane Acad Sci Ser France 270:1901
44. Nadaf YF, Mulimani BG, Gopal M, Inamdar SR (2004) J Mol Struct (Theochem) 678:177
45. Srividya N, Ramamurthy P, Ramakrishnan VT (1997) Spectrochim Acta 53A:1743
46. Lang K, Kubat P, Lhotak P, Mosinger J, Wagnerova DM (2001) J Photochem Photobio 74:558
47. Ikeda A, Suzuki Y, Yoshimura M, Shinkai S (1998) Tetrahedron 54:2497
48. Benesi HA, Hildebrand JH (1949) J Am Chem Soc 71:2703

49. Cervero M, Mendicuti F (2000) J Phys Chem 104 B:1572
50. Yand J, Huang F, Wang M, Wu X, Sun C (2002) Spectrochim Acta 58A:1775
51. Subhani MS, Bhatti NK, Mohammad M, Khan AY (2000) Turk J Chem 24:223
52. Velasco J, Guardado P, Carmona C, Munzo MA, Balon M (1998) J Chem Soc Faraday Trans 94:1469
53. Lee BS, Dutta PK (1989) J Phys Chem 93:5665
54. Shinkai S, Ikeda A (1999) Pure Appl Chem 71:275
55. Caciuffo R, Francescangeli O, Melone S, Prager M, Ugozzoli F, Andreetti CD, Amoretti G, Coddens G, Blank H (1992) Physica B 180 &181:691
56. Leigh DA, Linnane P, Prichard RG, Jackson G (1994) J Chem Soc Chem Commun 389